

# Electronic band structure and chemical bonding in the novel antiperovskite $\text{ZnCNi}_3$ as compared with 8-K superconductor $\text{MgCNi}_3$ .

I.R. Shein\*, K.I. Shein, N.I. Medvedeva and A.L. Ivanovskii  
*Institute of Solid State Chemistry, Ural Branch of the  
 Russian Academy of Sciences, 620219, Ekaterinburg, Russia*

Energy band structure of the discovered ternary perovskite-like compound  $\text{ZnCNi}_3$  reported by Park et al (2004) as a non-superconducting paramagnetic metal was investigated using the FLMTO-GGA method. The electronic bands, density of states, Fermi surface, charge density and electron localization function distributions for  $\text{ZnCNi}_3$  are obtained and analyzed in comparison with the isoelectronic and isostructural 8K superconductor  $\text{MgCNi}_3$ . The effect of external pressure on the electronic states of  $\text{ZnCNi}_3$  and  $\text{MgCNi}_3$  is studied.

\* E-mail: shein@ihim.uran.ru

PACS numbers: 74.70.-b, 71.20.-b

The interest in the properties of the perovskite - like intermetallic systems has increased in the past years due to the recent discovery of superconductivity (SC) with transition temperature up to 8 K in the perovskite - like  $\text{MgCNi}_3$  by<sup>1</sup>. Several factors attach special significance to this discovery. Among perovskite - like phases, the  $\text{MgCNi}_3$  is the first oxygen-free superconductor. Among low-temperature superconductors, the  $\text{MgCNi}_3$  also occupies a special place. Because large content of Ni in  $\text{MgCNi}_3$ , it is expected that this material is in close proximity to ferromagnetism. The occurrence of superconductivity in this system is very unusual; this makes it similar to the discovered recently ferromagnetic superconductors, and  $\text{MgCNi}_3$  can be treated as an "intermediate phase" between the groups of conventional nonmagnetic and ferromagnetic superconductors. Since 2001, the properties of the  $\text{MgCNi}_3$  have been investigated in detail, see review<sup>2</sup>. However till now the nature of the pairing mechanism in this SC material is still controversial. On the one hand, the temperature dependence of specific heat, the NMR data and some theoretical estimations allow to suggest that  $\text{MgCNi}_3$  is a classical superconductor with isotropic s-wave BCS pairing. On the other hand, a microwave impedance and tunneling data can be considered as arguments of non-s-wave behavior.

The great attention has been paid to influence of the doping effects on  $\text{MgCNi}_3$  properties, and various solid solutions such as  $\text{MgCNi}_{3-x}\text{M}_x$  ( $M = \text{d-metals}$ ) are synthesized.

Quite recently, Park et al<sup>3</sup> have carried out a synthesis of novel  $\text{ZnCNi}_3$  phase by solid-state route and characterized by X-ray powder diffraction (XRD), dc-resistivity, magnetization and specific heat measurements. It was found that  $\text{ZnCNi}_3$  is isostructural with 8 SC  $\text{MgCNi}_3$  however remains a paramagnetic metal up to  $T < 2$  K. The absence of superconductivity in  $\text{ZnCNi}_3$  is interpreted<sup>3</sup> within the BCS framework in terms of the reduction in lattice constant  $a$  (about 3.6 %) will lead to sharply decrease in the total density of states at the Fermi level  $N(E_F)$ .

In this report, we are focusing on the electronic band structure and chemical bonding in  $\text{ZnCNi}_3$  in comparison with  $\text{MgCNi}_3$  by means of a scalar relativistic full-potential linear muffin-tin method (FLMTO) with the generalized gradient approximation (GGA) for correlation and exchange effects<sup>4,5</sup>. In order to analyze the bonding effects, we have calculated the electronic localization function (ELF<sup>6,7</sup>) and charge density ( $\rho$ ) distributions. The interatomic bond indices (crystal orbital overlap populations - COOPs) were also estimated using simple band structure tight-binding EHT approach<sup>8</sup>.

$\text{ZnCNi}_3$  has the cubic perovskite-like structure (space group  $\text{Pm}\bar{3}\text{m}$ ) consisting of Zn at the corners, C at the body center, and Ni at the face centers of the cube. The atomic positions are Ni: 3 (0.5,0.5,0); Zn: 1a (0,0,0); C: 1b (0.5,0.5,0.5). At the first stage the lattice parameter of  $\text{ZnCNi}_3$  has been optimized ( $a=0.3747$  nm). We find that this value is about 2.3% overestimated as compared with experiment ( $0.366$  nm<sup>3</sup>) as is typical of generalized gradient calculations within the LDA.

The energy bands, total and site-projected  $l$ -decomposed densities of states (DOS) for  $\text{ZnCNi}_3$  and  $\text{MgCNi}_3$  are shown in Figs. 1 and 2, respectively. The valence band in  $\text{ZnCNi}_3$  is derived basically from the 15 Ni3d and 3 C2p states filled by 34 electrons (Fig. 1). C2s and Zn

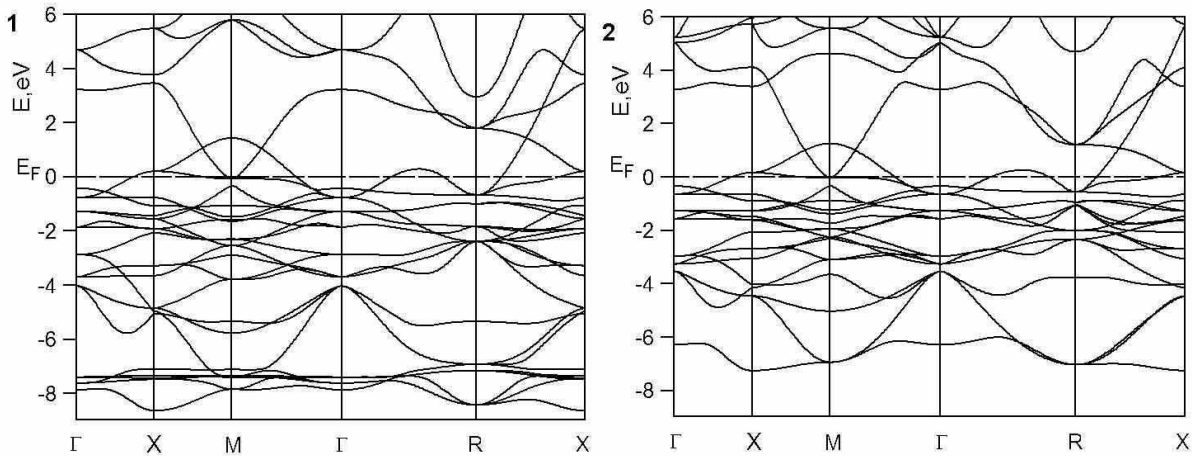


FIG. 1: . Energy bands for  $\text{ZnCNi}_3$  (1) and  $\text{MgCNi}_3$  (2).

states play a minor role in this area. The C 2p states are hybridized with Ni3d, and are located below nine near-Fermi bands which are formed mainly from Ni3d states. From these bands three are bonding, three nonbonding, and three antibonding bands. Two of antibonding  $\pi$ -bands cross  $E_F$ . The upper band produces hole-like two - sheet Fermi surface centered at the X point and ellipse-like along the  $\Gamma$ -R line, Fig 3. The Fermi surface involves also electron-like sheets around  $\Gamma$  point and along the R-M line generated by the lower band. As is seen from Fig. 1, energy bands of isostructural and isoelectronic phase  $\text{MgCNi}_3$  are quite similar.

The most remarkable feature of the DOS is a narrow intense peak in the vicinity of the Fermi level (Fig. 2). This peak is associated with the quasi-flat Ni 3d band aligned along the X-M and M- $\Gamma$  directions in the Brillouin zone. The Fermi level is located at the high-energy slope of the above peak. The maximum contribution ( 84.4 %, Table 1) to the density of states at the Fermi level  $N(E_F)$  is made by the Ni 3d states, and these states are responsible for metallic properties of the material.

Let's consider the chemical bonding in  $\text{ZnCNi}_3$ . The ELF distribution for the section through Zn, C and Ni atoms in  $\text{ZnCNi}_3$  is presented in Fig. 4. According to spatial organization of this scalar function  $\Lambda^{6,7}$  which describes the local kinetic energy, the ELF can take values in the interval  $0 < \Lambda < 1$ . Here the value  $\Lambda = 1$  corresponds to perfect localization and  $\Lambda = 0.5$  to the case of a free electron gas. For  $\text{ZnCNi}_3$  a maximum value of the  $\Lambda$  in the range about 0.8 around the carbons indicate an anionic state of these atoms in the crystal. The presence of a local minimum of the  $\Lambda$  on the line connecting Ni and C atoms may be interpreted as covalent bonding. Metallic bonding, which is an intermediate case between the covalent and the ionic bonding, is described by a rather uniform  $\Lambda$  distribution in region between Ni and Zn atoms. Corresponding electron density distributions  $\rho$  can be well distinguished on the charge map, Fig. 4.

In order to analyze in detail the bonding picture in  $\text{ZnCNi}_3$  we have calculated the crystal orbital overlap populations (COOPs) values by means of simple tight binding band structure method within the extended Huckel theory (EHT) approximation<sup>8</sup>. The results obtained indicate (Table 2) that the Ni-C covalent interactions are the strongest bonds in  $\text{ZnCNi}_3$ , whereas other bond types (Ni-Zn and Zn-C) are appeared on the order less. Interestingly, that the Ni-C COOP values in  $\text{ZnCNi}_3$  are about 3.4% weaker as compared with  $\text{MgCNi}_3$ , in spite of the fact that Ni-C distances are shorter. On the contrary, the degree of covalency of Ni-Zn and Zn-C bonds in  $\text{ZnCNi}_3$  as compared with Ni-Mg and Mg-C bonds in  $\text{MgCNi}_3$  grows.

Let's address to relation between electronic structure and superconductivity. As is known, in the BCS strong coupling limit,  $T_c$  is expressed by the McMillan formula<sup>9</sup>:  $T_c \sim \langle \omega \rangle \exp f(\lambda)$ , where  $\langle \omega \rangle$  represents an averaged phonon frequency, the coupling constant  $\lambda = N(E_F) \langle I^2 \rangle / M \langle \omega^2 \rangle$ ,  $\langle I^2 \rangle$  - frequency is an averaged electron-ion matrix element squared, M is an atomic mass, and  $N(E_F)$  is the density of states at the Fermi level.

Our FLMTO-GGA calculations showed, that the  $N(E_F)$  values for  $\text{MgCNi}_3$  (5.399) and  $\text{ZnCNi}_3$

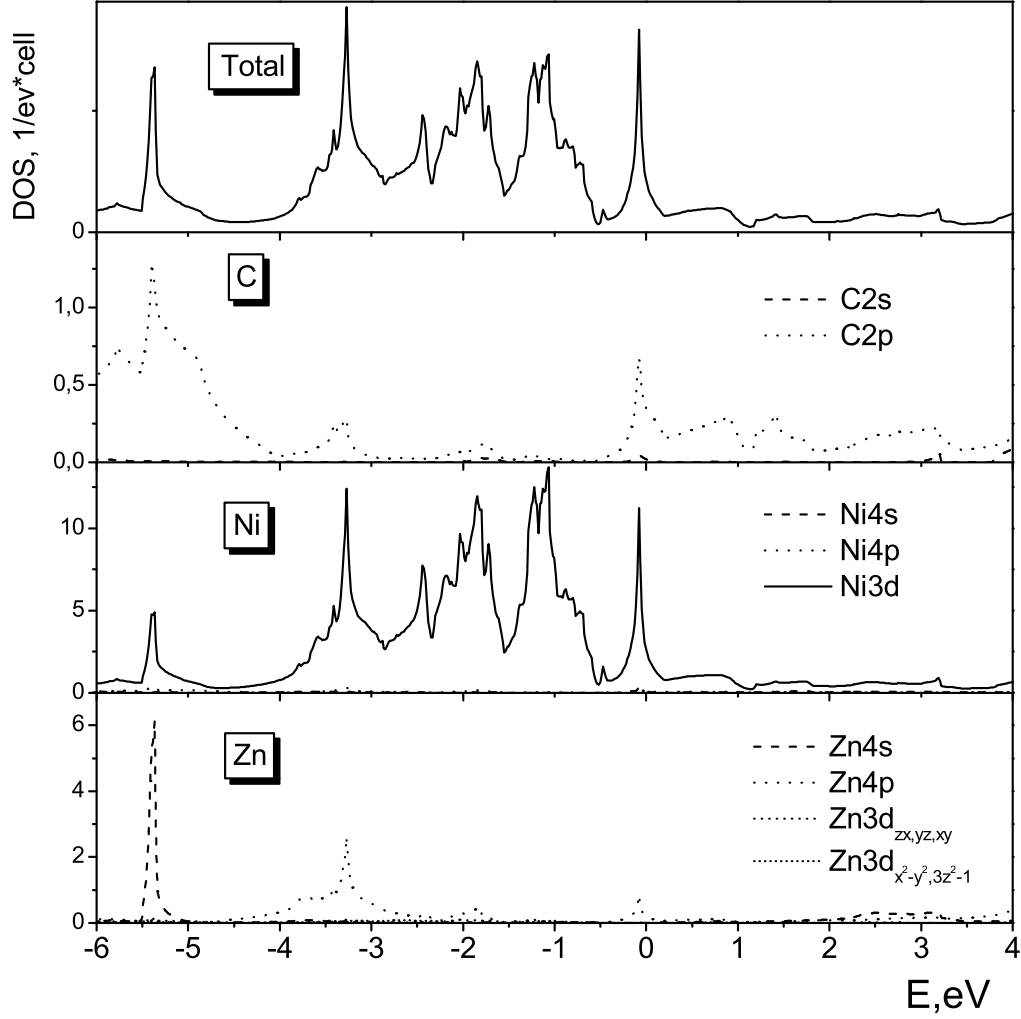


FIG. 2: . Total and site- projected  $l$ - decomposed densities of states for  $\text{ZnCNi}_3$ .

(4.401 states/eV) differ less, than on 18.5 %. Thus, our data sharply differ from crude estimations of authors<sup>3</sup>, according to which the absence of superconductivity in  $\text{ZrCNi}_3$  can be achieved if the ratio  $N(E_F)[\text{ZnCNi}_3]/N(E_F)[\text{MgCNi}_3] \sim 0.41$ . As one of the possible reasons of rapid reduction of  $N(E_F)$  the proximity of the Fermi energy to a large near-Fermi peak in the DOS (van Hove singularity) is assumed<sup>3</sup>. It was supposed, as  $\epsilon$  decreases, the broadening of van Hove singularity peak is accompanied by the fast decreasing in  $N(E_F)$ .

To check this assumption we have analyzed the pressure dependence of the near-Fermi DOSs for  $\text{MgCNi}_3$  and  $\text{ZnCNi}_3$ . The results obtained indicate (Table 1) that with growth of external pressure (reduction in lattice parameter) the  $N(E_F)$  both for  $\text{MgCNi}_3$  and  $\text{ZnCNi}_3$  decreases monotonically, however the ratio  $N(E_F)[\text{ZnCNi}_3]/N(E_F)[\text{MgCNi}_3]$  varies a little. For  $\text{MgCNi}_3$  these results are in agreement with earlier theoretical and experimental findings<sup>10</sup>, according to which external pressure leads to  $T_c$  reduction as result of  $N(E_F)$  decreasing.

In conclusion, we have presented the first principle band structure calculations for the newly discovered ternary intermetallic perovskite-like  $\text{ZnCNi}_3$  in comparison with isoelectronic and isostructural 8 superconductor  $\text{MgCNi}_3$  performed by the FLMTO-GGA method. It was established that the general features of  $\text{ZnCNi}_3$  and  $\text{MgCNi}_3$  band structure and interatomic bonding

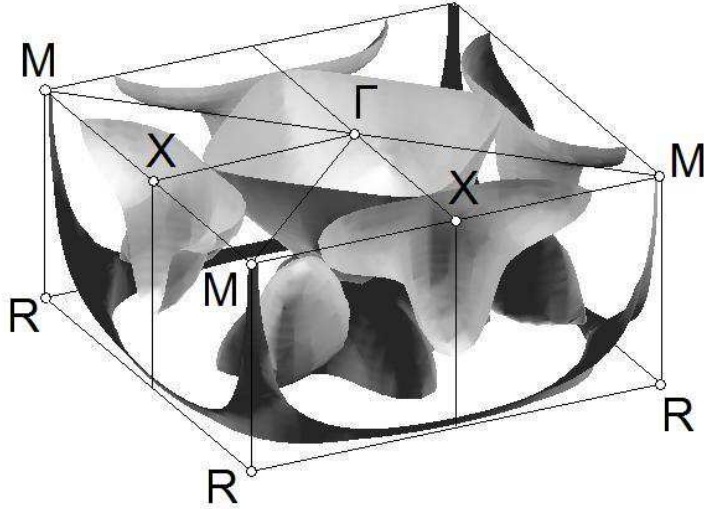


FIG. 3: Fermi surface for  $\text{ZnCNi}_3$ .

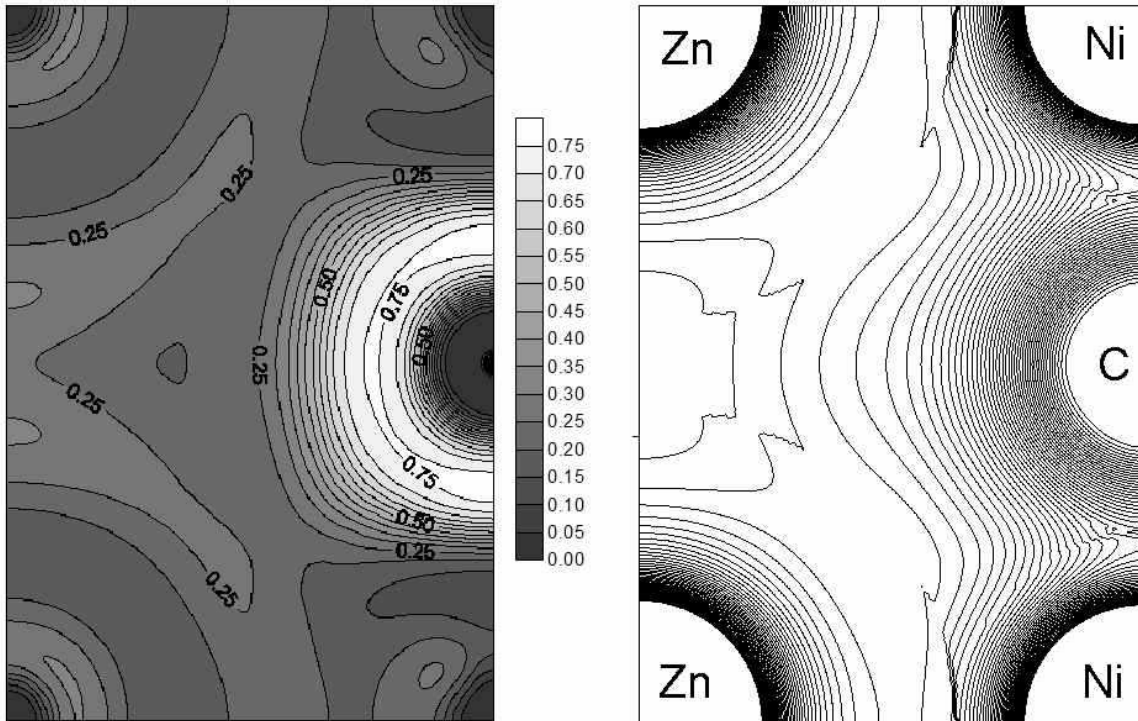


FIG. 4: ELF (left) and charge density contours (right) for the (110) section of  $\text{ZnCNi}_3$ .

are similar and can be briefly summarized as follows: there is a strong hybridization between the Ni-3d electrons and the C-2p states and thus carbon plays the crucial role of the mediator of electron hopping. Two of the (Ni3d - C2p)-like bands cross the Fermi level and contribute to conductivity. Remarkable feature of the DOS of these materials is a sharp peak below  $E_F$  arising from the  $\pi$  - antibonding Ni3d states. The  $N(E_F)$  is formed predominantly due to Ni3d states.

TABLE I: Total  $N(E_F)$  and site- projected l- decomposed densities of states at the Fermi level (states/eV cell) as function of external pressure (P, GPa) for antiperovskites  $ZnCNi_3$  and  $MgCNi_3$ .

P	293.7	232.6	182.0	140.2	105.7	77.5	54.4	35.6	20.3	8.1	0
C2s	0.019	0.019	0.019	0.019	0.019	0.019	0.020	0.020	0.020	0.020	0.021
C2p	0.306	0.309	0.312	0.314	0.318	0.323	0.328	0.333	0.337	0.342	0.345
Ni4s	0.055	0.056	0.056	0.056	0.056	0.056	0.057	0.058	0.059	0.060	0.060
Ni4p	0.097	0.095	0.094	0.092	0.091	0.089	0.089	0.087	0.086	0.085	0.085
Ni4d	2.907	2.985	3.064	3.095	3.177	3.255	3.355	3.456	3.539	3.644	3.716
Zn4s	0.003	0.003	0.003	0.003	0.003	0.003	0.003	0.003	0.003	0.003	0.003
Zn4p	0.163	0.162	0.162	0.158	0.157	0.155	0.145	0.151	0.153	0.153	0.153
Zn3d	0.025	0.024	0.024	0.023	0.022	0.022	0.021	0.020	0.020	0.019	0.019
<b><math>N(E_F)</math></b>	<b>3.575</b>	<b>3.654</b>	<b>3.734</b>	<b>3.758</b>	<b>3.843</b>	<b>3.923</b>	<b>4.027</b>	<b>4.128</b>	<b>4.217</b>	<b>4.325</b>	<b>4.401</b>
P	279.4	223.4	176.8	138.1	106.1	79.54	57.7	39.74	25.1	13.2	0
C2s	0.019	0.019	0.019	0.019	0.019	0.019	0.019	0.019	0.019	0.019	0.020
C2p	0.377	0.379	0.379	0.382	0.384	0.387	0.390	0.392	0.394	0.395	0.403
Ni4s	0.084	0.083	0.080	0.080	0.079	0.080	0.080	0.081	0.081	0.080	0.083
Ni4p	0.120	0.118	0.114	0.112	0.110	0.109	0.108	0.106	0.104	0.101	0.099
Ni4d	3.683	3.746	3.731	3.804	3.882	4.005	4.108	4.215	4.315	4.367	4.607
Mg3s	0.001	0.001	0.001	0.001	0.001	0.001	0.001	0.001	0.001	0.001	0.000
Mg3p	0.190	0.186	0.177	0.173	0.172	0.174	0.175	0.173	0.172	0.167	0.165
Mg3d	0.032	0.031	0.030	0.028	0.027	0.027	0.026	0.025	0.024	0.023	0.022
<b><math>N(E_F)</math></b>	<b>4.507</b>	<b>4.563</b>	<b>4.530</b>	<b>4.598</b>	<b>4.675</b>	<b>4.803</b>	<b>4.907</b>	<b>5.012</b>	<b>5.111</b>	<b>5.154</b>	<b>5.399</b>

TABLE II: The COOPs (electron/bond) of interatomic bonds in  $ZnCNi_3$  and  $MgCNi_3$  according tight-binding EHT estimations.

$ZnCNi_3$			$MgCNi_3$		
Bonds	Distances,nm	COOP's	Bonds	Distances,nm	COOP's
Ni-C	0.1876	0.2898	Ni-C	0.1898	0.2999
Ni-Zn	0.2653	0.0744	Ni-Mg	0.2684	0.0393
Zn-C	0.3249	0.0056	Mg-C	0.3287	0.0017

According to ELF and charge density analysis, the bonding in  $ZnCNi_3$  is of "mixed" character: the ionic contribution (due to additional charge localization on C atoms) in this phase coexists with Ni-C covalent bonding and a metallicity provided by the delocalized Ni states. The simple TB estimations showed also that the replacement  $Mg \rightarrow Zn$  in perovskite-like phase results in the population redistribution between separate bond types thus the strongest Ni-C bonds in  $ZnCNi_3$  as compared with  $MgCNi_3$  are weaker in spite of the fact that Ni-C distances are shorter. Our LMTO-GGA band structure calculations show, that to explain the absence of superconductivity in  $ZnCNi_3$  based only on the electronic factor (reduction in  $N(E_F)$ ) as compared with  $MgCNi_3$ <sup>3</sup> is impossible. Obviously, the important role in the observed non-superconducting state in  $ZnCNi_3$  will belong to the changes in phonon frequencies as well as to possible structural and chemical defects. For example, the effect of vacancies on the value of  $T_c$  is noticeable for  $MgCNi_3$ .

Acknowledgement.

This work was supported by the RFBR, grants 02-03-32971 and 04-03-32082.

- 
- <sup>1</sup> T. He, Q. Huang, A.P. Ramirez, Y. Wang, K.A. Regan, N. Rogado, M.A. Hayward, M.K. Haas, J.S. Slusky, K. Inumaru, H.W. Zandbergen, N.P. Ong, R.J. Cava. *Nature (London)*, **411** (2001) p.54.
  - <sup>2</sup> A.L. Ivanovskii, *Phys. Solid State*, **45** (2003) p.1829.
  - <sup>3</sup> Min-Seok Park, Jin-Soo Giim, Soo-Hyeon Park, Y.W. Lee, S. I. Lee, E. J. Choi. *Supercond. Sci. Technol.*, **17** (2004) p.274.
  - <sup>4</sup> S.Y. Savrasov, *Phys. Rev.* **B54** (1996) p.16470.
  - <sup>5</sup> J.P. Perdew, K.Burke, M. Ernzerhof, *Phys. Rev. Lett.* **77** (1996) p.3865.
  - <sup>6</sup> A.D. Becke, K.E. Edgecombe. *J. Chem. Phys.* **92** (1990) p.5397.
  - <sup>7</sup> A. Savin, O. Jepsen, J. Flad, R. Nesper, H. Preuss, H.G. Schering, *Andew. Chem. Intern. Ed.*, **31** (1991) p.187.
  - <sup>8</sup> R. Hoffmann, *Solids and surfaces: a chemist's view of bonding in extended structures*, VCH: N.Y., 1988.
  - <sup>9</sup> W. L. McMillan, *Phys. Rev.* **167** (1968) p.331.
  - <sup>10</sup> T. G. Kumary, J. Janaki, A. Mani, S. M. Jaya, V. S. Sastry, Y. Hariharan, T. S. Radhakrishnan, M. C. Valsakumar, *Phys. Rev.* **B66** (2002) p.064510.